

Nanoscale Contact Mechanics between Two Grafted Polyelectrolyte Surfaces

Raftari, Maryam; Zhang, Zhenyu; Carter, Steven; Leggett, Graham J.; Geoghegan, Mark

DOI:

[10.1021/acs.macromol.5b01540](https://doi.org/10.1021/acs.macromol.5b01540)

Document Version

Peer reviewed version

Citation for published version (Harvard):

Raftari, M, Zhang, Z, Carter, S, Leggett, GJ & Geoghegan, M 2015, 'Nanoscale Contact Mechanics between Two Grafted Polyelectrolyte Surfaces', *Macromolecules*, vol. 48, no. 17, pp. 6272-6279.
<https://doi.org/10.1021/acs.macromol.5b01540>

[Link to publication on Research at Birmingham portal](#)

General rights

Unless a licence is specified above, all rights (including copyright and moral rights) in this document are retained by the authors and/or the copyright holders. The express permission of the copyright holder must be obtained for any use of this material other than for purposes permitted by law.

- Users may freely distribute the URL that is used to identify this publication.
- Users may download and/or print one copy of the publication from the University of Birmingham research portal for the purpose of private study or non-commercial research.
- User may use extracts from the document in line with the concept of 'fair dealing' under the Copyright, Designs and Patents Act 1988 (?)
- Users may not further distribute the material nor use it for the purposes of commercial gain.

Where a licence is displayed above, please note the terms and conditions of the licence govern your use of this document.

When citing, please reference the published version.

Take down policy

While the University of Birmingham exercises care and attention in making items available there are rare occasions when an item has been uploaded in error or has been deemed to be commercially or otherwise sensitive.

If you believe that this is the case for this document, please contact UBIRA@lists.bham.ac.uk providing details and we will remove access to the work immediately and investigate.

Nanoscale Contact Mechanics between Two Grafted Polyelectrolyte Surfaces

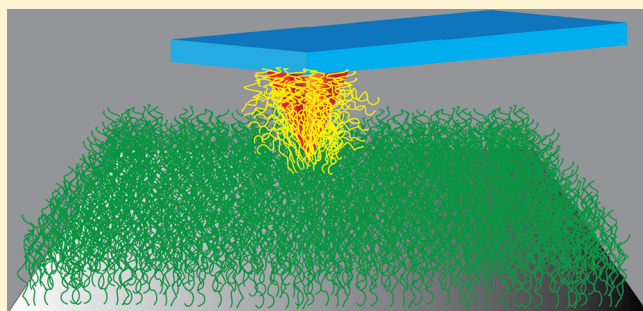
Maryam Raftari,[†] Zhenyu J. Zhang,^{‡,†} Steven R. Carter,[†] Graham J. Leggett,[‡] and Mark Geoghegan^{*,†}

[†]Department of Physics and Astronomy, University of Sheffield, Hounsfield Road, Sheffield S3 7RH, U.K.

[‡]Department of Chemistry, University of Sheffield, Brook Hill, Sheffield S3 7HF, U.K.

Supporting Information

ABSTRACT: The adhesive and frictional behavior of end-grafted poly[2-(dimethylamino)ethyl methacrylate] (PDMAEMA) films (brushes) in contact with atomic force microscope tips from which PDMAEMA and poly(methacrylic acid) (PMAA) were grafted has been shown to be a strong function of pH in aqueous solution. The interaction between the brush-coated surfaces is determined by a combination of electrostatic and noncovalent interactions, modulated by the effect of the solvation state on the brush and the resulting area of contact between the probe and the surface. For cationic PDMAEMA–PDMAEMA contacts at low pH, the brushes are highly solvated; a combination of electrostatic repulsion and a high degree of solvation (leading to a significant osmotic pressure) leads to a small area of contact, weak adhesion, and energy dissipation through plowing. As the pH increases, the electrostatic repulsion and the osmotic pressure decrease, leading to an increase in the area of contact and a concomitant increase in the strength of adhesion through hydrophobic interactions; as a consequence, the friction–load relationship becomes nonlinear as shear processes contribute to friction and the mechanics are fitted by DMT theory and, at higher pH, by the JKR model. For PDMAEMA–PMAA, the electrostatic interaction is attractive at neutral pH, leading to a large adhesion force, a large area of contact, and a nonlinear friction–load relationship. However, as the pH becomes either very small or very large, a significant charge is acquired by one of the contacting surfaces, leading to a large amount of bound solvent and a significant osmotic pressure that resists deformation. As a consequence, the area of contact is small, adhesion forces are reduced, and the friction–load relationship is linear, with energy dissipation dominated by molecular plowing.



1. INTRODUCTION

Polymers end-grafted to surfaces are known as brushes and have assumed a technological importance because of real and potential applications in adhesion,^{1–3} lubrication and friction,^{4–7} and controlled cell growth⁸ and biocompatibility.⁹ Charged polymers, however, have a great deal of promise in these areas because their properties can be readily controlled by environmental pH and salt.^{4,10–17} The combination of positively and negatively charged polyelectrolytes in particular is particularly powerful because strong adhesion between the two occurs at intermediate pH. For example, the layer-by-layer technique provides polymer multilayers of controlled thickness,¹⁸ but the adhesion between oppositely charged polyelectrolytes can be reversed by a simple pH change.^{13,14} The interaction between charged polymers is of further interest because this situation includes two lubricating surfaces. For polymers of the same charge, the nature of the process is dependent on the relative motion of the two surfaces, the force applied, and the physical properties of the polymers (e.g., molar mass).¹⁹ The pH dependence of the interaction between polymers of the same charge is important because the lubricity of the polymers depends on their charged status. However, the

role of counterions is also important and can even facilitate an attraction between layers of the same charge.²⁰ Simply because both surfaces are good lubricants in water does not imply that they must be assumed to be lubricious when brought together. For the case of polyelectrolytes of opposite charge, the underlying mechanism for the adhesive interaction is unclear. Hydrogen bonds are known to be important in pH-dependent polymer interactions²¹ and even to control pH-switchable adhesion,²² and the relative roles of electrostatic and hydrogen bonding in the adhesion between oppositely charged polyelectrolytes have not been confirmed.¹⁴ The contact mechanics between charged surfaces provides a means to test the nature of these polymer–polymer interactions. For both situations (polycation with polycation or polycation with polyanion), the interaction will be strongly dependent upon pH.

The controllable lubricity of polyelectrolytes can be studied using friction force microscopy (FFM),^{23–26} a scanning probe microscopy (SPM) technique that allows the nanotribological

Received: July 12, 2015

characteristics of a surface to be probed using a well-defined nanoscale atomic force microscope probe (AFM tip) that may be chemically modified to control its interaction with the surface.^{27–31} Some FFM experiments have been performed with a colloidal probe,^{32–34} which can provide a better defined surface than that offered by an AFM tip. However, an AFM tip is preferred because the goal here is to understand single asperity brush–brush contacts. Because SPM experiments can be performed in solution, FFM is ideal for the investigation of the adhesion and friction of end-grafted polyelectrolytes.¹⁵ Control and understanding of friction in polymer brush contacts in general has been the subject of significant research in recent years, particularly because polymer brushes are a practical means of altering the tribological properties of a surface.^{5,35–37} In an earlier study,¹⁵ it was shown that the frictional interaction between poly[2-(dimethylamino)ethyl methacrylate] (PDMAEMA, a polycation) brushes and AFM tips depends strongly on the environmental pH, with a linear friction–load relationship observed at the extremes of pH, and adhesion-dominated behavior, consistent with either DMT or JKR mechanics observed at intermediate pH. Importantly, whether or not DMT or JKR behavior was observed depended not only on the environmental pH but also on the chemical nature of the AFM tip.

The mechanism of interaction between an AFM tip and a polymer brush is not trivial. Different types of friction–load relationships have been observed previously on a range of polymer brush systems. Linear relationships, described by Amontons' law,³⁸ which is a multiasperity model indicates that the applied load, N , rather than the area of contact, A , is the determining factor, and the frictional force is given by

$$F = \mu N \quad (1)$$

where μ is the coefficient of macroscopic friction. Linear relationships have been observed in different polymer brush systems.^{15,35,39,40} However, with an AFM tip, single-asperity contact mechanics would be expected and have indeed been observed.^{15,17,41–43}

Single-asperity models of contact mechanics can be split into two extremes. Softer materials are more able to conform to a surface than those with a larger modulus, and this situation is described by the Johnson–Kendall–Roberts (JKR) model,⁴⁴ which is given by

$$A = \pi \left(\frac{R}{K} (N + 3\pi\gamma R + \sqrt{6\pi\gamma RN + (3\pi\gamma R)^2}) \right)^{2/3} \quad (2)$$

for a hemispherical (radius R) contact with a planar surface. Here γ is the interfacial energy (thermodynamic work of adhesion), and K is the effective elastic modulus of the medium perturbed by the contact. A model proposed by Derjaguin, Muller, and Toporov⁴⁵ caters for more rigid interfaces and is given by

$$A = \pi \left(\frac{R}{K} \right)^{2/3} (N + 4\pi\gamma R)^{2/3} \quad (3)$$

Both the DMT and JKR models reduce to the same (Hertz) model⁴⁶ when $\gamma = 0$. It is not the case that a choice must be made between JKR or DMT; a transition parameter,⁴⁷ α , can be used as a scale between JKR ($\alpha = 1$) and DMT ($\alpha = 0$) to evaluate the contact mechanics. This transition parameter relates the contact radius, a (where $A = \pi a^2$), to the applied load by

$$a = a_0 \left(\frac{\alpha + \sqrt{1 - N/N_{PO}}}{1 + \alpha} \right)^{2/3} \quad (4)$$

where N_{PO} is the force required to separate the two components, known as the pull-off force.

Recently, the frictional force of single asperity contacts has been shown to comprise a regime of low adhesion, when the load applied to the surface, N , dominates and molecular deformation “plowing” occurs, and an area-dependent high adhesion term, when the surface is sheared by the tip.^{23,48,49} During the friction measurement, work is done by perturbing the conformation of the brush; the brush then returns to its equilibrium conformation via the dissipation of energy as heat. Here, the load-dependent term represents (irrecoverable) energy dissipation through plowing. However, the shear-dependent term, characterized by a surface shear strength τ , represents the stress required to maintain a sliding contact. These can be synthesized into a frictional force dependent upon two terms:^{50,51}

$$F = \mu(N + N_{PO}) + \tau\pi \left(\frac{R(N + N_{PO})}{K} \right)^{2/3} \quad (5)$$

Equation 5 has already been shown to explain qualitatively the single asperity contact mechanics of a polyzwitterionic brush.¹⁷ Both load-dependent and area-dependent terms contribute to the overall friction force, depending on the solvation state of the polymer brush.

In this work, experiments are described in which polyelectrolyte brush layers were grown from AFM tips, chemically modified with a coating of an initiator layer. The frictional properties of these brushes interacting with planar brushes of the same or opposite charge were monitored as a function of pH. As in the earlier work,¹⁵ it is shown that the pH affects whether or not DMT or JKR behavior is observed, and again Amontons-like behavior is observed at the extremes of pH.

2. EXPERIMENTAL SECTION

2.1. Materials. Silicon wafers (boron doped, 0–100 Ω cm, and (100) orientation) were purchased from Prolog Semicon (Ukraine). Copper(I) chloride (99.999%), copper(II) bromide (99.999%), [11-(2-bromo-2-methyl)propionyloxy]undecyltrichlorosilane, *p*-toluenesulfonic acid monohydrate (98.5%), pentamethyldiethylenetriamine (99%), *t*-butyl methacrylate (99%), 1,4-dioxane (99.5%), dry toluene (99.8%), 2-(dimethylamino)ethyl methacrylate ($C_8H_{15}NO_2$), HCl (37%), and NaOH (>97%) were all purchased from Aldrich and used as received. HPLC grade acetone, methanol, acetic acid, and triethylamine were purchased from Fisher Scientific. 2,2'-Dipyridyl (99%) was purchased from Acros.

2.2. Brush Synthesis and Modification of the AFM Cantilever. PDMAEMA brushes were grafted from silicon substrates and silicon nitride AFM tips by atom transfer radical polymerization (ATRP). Here, the initiator was immobilized on the substrate, followed by the synthesis of the polymer brush layer.

To immobilize the initiator, the clean silicon wafer and AFM tip were immersed for 6 h in 20 mL of dry toluene solution containing 50 μ L of [11-(2-bromo-2-methyl)propionyloxy]undecyltrichlorosilane (initiator). When coated, the substrates and AFM tip were rinsed with toluene and then dried under nitrogen gas. The AFM tips before modification were nonconductive silicon nitride triangular probes (MLCT, Bruker) with nominal spring constant 0.065 N m⁻¹ and radius 20 nm.

To prepare cationic monomer solutions for ATRP, 2,2'-dipyridyl (0.225 g), CuCl (0.0624 g), and CuBr₂ (0.0084 g) were added

184 together as catalysts. These catalysts were dissolved by adding
 185 degassed acetone (15.9 mL) and 1.5 mL of deionized water. The
 186 ATRP monomer solution was finally prepared by adding the 10.8 mL
 187 of 2-(dimethylamino)ethyl methacrylate (DMAEMA) to the catalyst
 188 solution. Finally, 20 mL of the ATRP solution was injected into a cell
 189 (sealed under nitrogen), which contained the initiator-coated silicon
 190 wafer and AFM tip. The PDMAEMA sample and the PDMAEMA-
 191 coated AFM tip were removed and rinsed with methanol after 16 h.
 192 AFM tips modified to contain a poly(methacrylic acid) (PMAA)
 193 brush were prepared in three stages. First, the trichlorosilane initiator
 194 monolayer was prepared in the same way as for the PDMAEMA
 195 brushes, then the synthesis of poly(*tert*-butyl methacrylate) brushes
 196 were synthesized by ATRP, and finally the poly(*tert*-butyl
 197 methacrylate) was hydrolyzed to produce PMAA brushes.

198 Poly(*tert*-butyl methacrylate) brushes were synthesized using ATRP
 199 on the surface-initiated AFM tip. Here, 20 mL of *tert*-butyl
 200 methacrylate, 10 mL of anhydrous dioxane, and 200 μ L of
 201 pentamethyldiethylenetriamine were added together. Then 20 mL of
 202 this ATRP solution was injected to the cell containing the initiated tip
 203 and wafer and 0.1 g of CuCl (I). This cell was left on a heater at 50 $^{\circ}$ C
 204 for \sim 18 h. Finally, the coated tips and surfaces were rinsed with 1,4-
 205 dioxane and acetic acid. For hydrolysis, 0.2 M of *p*-toluenesulfonic acid
 206 and 10 mL of 1,4-dioxane were added over the coated tip in the cell
 207 and heated at 100 $^{\circ}$ C for 24 h. After hydrolysis, the PMAA-coated tips
 208 were removed and rinsed with 1,4-dioxane and ethanol. PMAA
 209 brushes were also grown from planar silicon surfaces using the same
 210 methodology in order to characterize the thickness of the films.

211 **2.3. Brush Characterization.** The average thickness of the PMAA
 212 and PDMAEMA films was determined by spectroscopic ellipsometry
 213 with an M-2000 spectroscopic ellipsometer (J.A. Woollam) for both
 214 dry brushes and those immersed in different pH solutions.
 215 Ellipsometry measurements were taken using wavelengths from 200
 216 to 1000 nm, and the data were fitted using the analysis software
 217 WVASE32 (J.A. Woollam). The ellipsometric thicknesses of the
 218 PMAA and PDMAEMA brushes were first measured to be about 58
 219 and 64 nm, respectively, in the dry state. X-ray photoelectron
 220 spectroscopy (XPS) was used to monitor each stage of the process on
 221 the planar surfaces and AFM tips using a Kratos Axis Ultra
 222 spectrometer. A monochromated 150 W Al $K\alpha$ source was used to
 223 acquire the spectra under an $\sim 10^{-6}$ Pa vacuum. All samples were left
 224 overnight at room temperature prior to analysis. Data were first
 225 recorded at a pass energy of 160 eV while high-resolution C(1s),
 226 O(1s), and N(1s) scans were recorded at a pass energy of 20 eV with a
 227 step size of 0.1 eV. Data were analyzed using CasaXPS software, and
 228 quantification was realized using the default Kratos RSF (relative
 229 sensitivity factor) library. Carbon spectra were charge corrected
 230 according to the value of aliphatic carbon C(1s) at 285 eV. High-
 231 resolution scans were taken of C(1s), O(1s), and S(2p) peaks. These
 232 high-resolution peaks were fitted using a Gaussian–Lorentzian model.
 233 The fwhm was kept below 1.7 eV. To check the thickness of
 234 PDMAEMA brushes on the cantilever, a Carl Zeiss 1540XB scanning
 235 electron microscope (SEM) was used to take images from a brush-
 236 modified cantilever. Free (i.e., not grafted) PDMAEMA was
 237 synthesized following the same protocol as that for the grafted
 238 PDMAEMA and characterized by gel permeation chromatography,
 239 from which a molar mass of 39 kg/mol was determined.¹⁵ The grafting
 240 density of the PDMAEMA was thus determined to be 0.84 chains/
 241 nm². Since the synthesis of the poly(*tert*-butyl methacrylate) followed
 242 the same procedure, a similar grafting density can be assumed. Given a
 243 dry thickness of 58 nm, the PMAA molar mass can therefore be taken
 244 to be 42 kg/mol.

245 **2.4. Friction Force Microscopy Experiments.** A Digital
 246 Instruments Nanoscope IIIa Multimode atomic force microscope
 247 was used for friction force measurements operating in contact mode
 248 with a liquid cell/tip holder. FFM experiments were performed at a
 249 scan rate (constant tip speed of 2 μ m/s) of 1 Hz with 256 points per
 250 (1 μ m) line. The spring constants of PMAA- and PDMAEMA-coated
 251 cantilevers were calibrated by a Digital Instruments PicoForce module
 252 and its associated software, based on the method of Hutter and
 253 Bechhoeffer.⁵² The PDMAEMA-coated tips were determined to have a

spring constant of 0.073 N m⁻¹, and those for the PMAA-coated tips
 254 were 0.080 N m⁻¹. (The unmodified cantilevers had spring constants
 255 in the range 0.063–0.068 N m⁻¹, close to the nominal value.) The
 256 optical lever sensitivity of each brush-coated cantilever was calibrated
 257 at neutral pH before each set of experiments. The lateral force was
 258 calibrated using the wedge method,^{53–55} with the cantilever scanning
 259 across a calibration grating (TGF11, MikroMasch, Tallinn, Estonia). 260

The frictional behavior between the PDMAEMA brush and each
 261 AFM-coated tip was measured in deionized water and solution with
 262 different pH (pH = 1–12) by the addition of HCl or NaOH as
 263 appropriate. A pH meter was routinely used to monitor pH. Buffer was
 264 not used to stabilize pH because of the contribution of the increased
 265 ionic strength to shielding the charges in the polyelectrolyte layers. 266

3. RESULTS

3.1. **Brush Thickness.** The variation of thickness with pH
 267 (from 1 to 12) of both PDMAEMA and PMAA brushes in
 268 solution was measured by ellipsometry using an effective
 269 medium approximation⁵⁶ to account for the nonuniform
 270 concentration profile of these brushes. Discrepancies due to
 271 the dry and ellipsometric thicknesses measured in solution can
 272 be taken as being due to the assumptions made in calculating
 273 the thickness. The ellipsometric thickness data are shown in 274

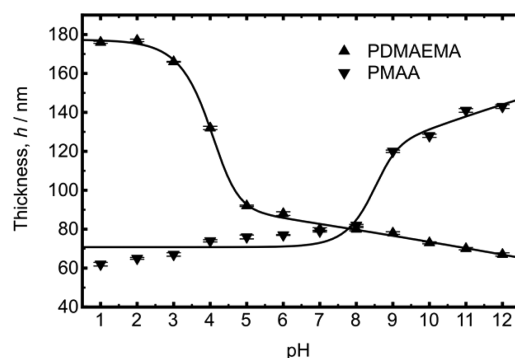


Figure 1. Ellipsometric characterization of the thickness of PDMAEMA and PMAA brushes grafted from planar silicon surfaces. The solid lines are fits to eq 6. The dry brush thicknesses (before immersion in solution) were respectively 64 and 58 nm. Error bars (not used in the fitting) were taken from 20 repeated measurements on different spots.

Figure 1. The solid lines in Figure 1 are fits to an empirical
 275 function for the thickness, given by 276

$$h = h_2 + \frac{h_1 - h_2}{2} \times \sqrt{\left(1 + \tanh\left(\frac{\text{pH} - \Delta_1}{\sigma_1}\right)\right)\left(1 + \tanh\left(\frac{\text{pH} - \Delta_2}{\sigma_2}\right)\right)} \quad (6)$$

where the parameters h_1 , h_2 , Δ_1 , Δ_2 , σ_1 , and σ_2 are fitting
 278 parameters with no substantive physical meaning. Equation 6
 279 exhibits an approximate form of the ellipsometry data, and its
 280 functional form enables a calculation of the thickness transition
 281 (equivalent to the pK_a) by setting its second derivative with
 282 respect to pH to be zero. As a result, the PDMAEMA brushes
 283 showed a thickness transition at pH = 4.1, which is significantly
 284 less than the pK_a of dilute aqueous solutions of PDMAEMA,
 285 where $\text{pK}_a = 7.0$ has been measured.⁵⁷ Similarly, the transition
 286 for PMAA was observed at 8.5, considerably greater than that
 287

for PMAA in dilute solution of 5.7.⁵⁸ (The uncertainty in these values is very small, but this uncertainty comes from taking eq 6 as axiomatic, when it is in fact empirical.) The shift in the conformational transition relative to the bulk pK_a is due to the effects of counterion condensation⁵⁹ in the brushes. The osmotic pressure of the counterions is significant, and the solution can lower its energy if the polyelectrolyte is partially neutralized. The effect of confinement on the charge distribution in polyelectrolyte brushes is dependent upon grafting density.⁶⁰

To measure the brush thickness on the AFM tip is considerably more challenging, but an indication of the presence of dry PDMAEMA brush and its thickness was obtained using a SEM. In Figure 2 a SEM image is shown of a

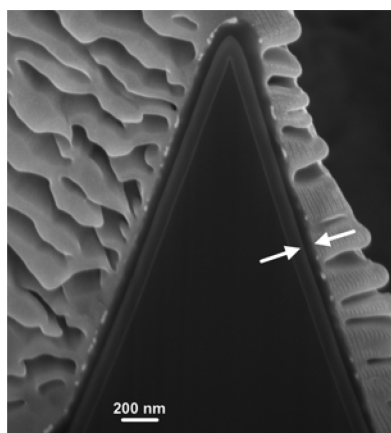


Figure 2. SEM image of PDMAEMA brush layer on the cantilever. The arrows indicate the location of the PDMAEMA brush. A layer of platinum, used to protect the brush layer during exposure to the gallium ion beam, is the outermost (wavy) structure shown in the micrograph.

cantilever from which a PDMAEMA brush was grown. A 5 nm gold layer was sputtered onto the brush and a 1 μm platinum strip subsequently attached. The platinum layer provides good protection for the brush from the milling process, which was performed with a 30 kV focused gallium ion beam. The thickness of 70 nm obtained using this procedure is consistent with the ellipsometry results.

3.2. Adhesion. The adhesive interactions were determined by checking the maximum force required in the retraction of the PDMAEMA- or PMAA-modified tips from contact with the PDMAEMA brush. Adhesion measurements were performed in solutions of different pH; 100 measurements were made for each pH. Figure 3 shows approach curves for the PDMAEMA- and PMAA-modified probes and the planar PDMAEMA brush layer immersed in solutions of different pH. It is revealing that for both samples the approach curves at intermediate pH indicate a stiffer interaction than at the extremes of pH, where the smaller slope indicates a smaller linear compliance. While surprising, these results do not contradict earlier data considering the effect of the polycation brush with different AFM tips coated with different surfaces.¹⁵ In those experiments, regardless of the nature of the surface, a linear friction–load relationship was observed at the extremes of pH. Under such conditions, the second area-dependent term in eq 5, associated with shearing (adhesive) contributions to friction, is small, and the load-dependent term dominates.

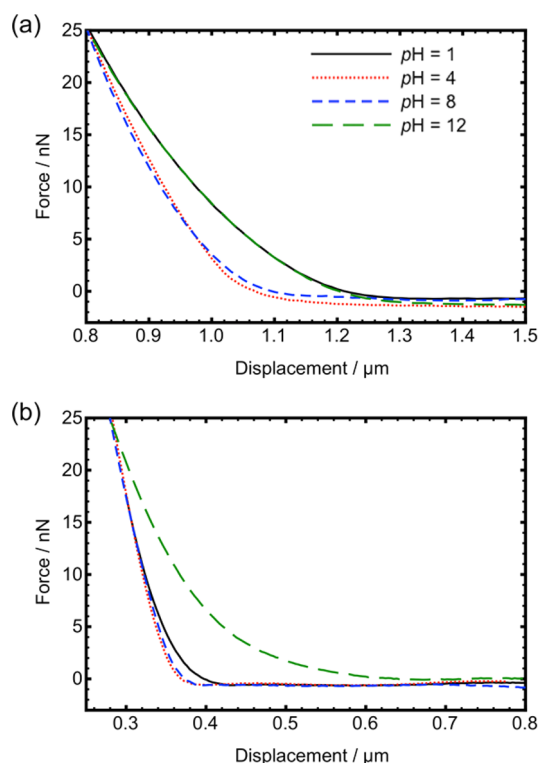


Figure 3. Approach curves for (a) PDMAEMA and (b) PMAA brush-coated tips to a PDMAEMA brush layer on a planar silicon substrate measured at four different pH values.

Retraction curves for the different systems are shown in Figure 4. The retraction curves, like the approach curves shown

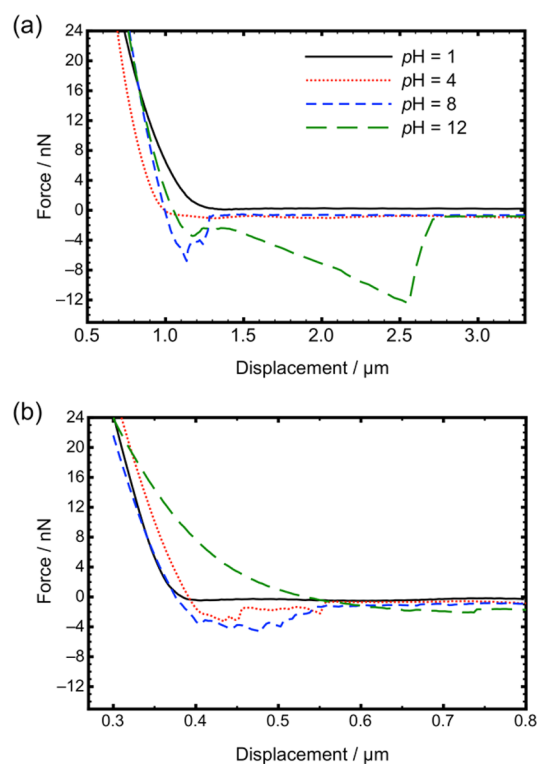


Figure 4. Retraction curves for (a) PDMAEMA and (b) PMAA brush-coated tips to a PDMAEMA brush layer on a planar silicon substrate measured at four different pH values.

in Figure 3, are presented as force as a function of displacement from the contact point, rather than force as a function of distance from a predefined zero in order to ensure reproducible and reliable interpretation of the data.⁶¹ The adhesion increases with pH for the PDMAEMA–PDMAEMA interaction, whereas it reaches a maximum at pH = 6 for the PMAA–PDMAEMA system (Figure 5). The maximum adhesion values for the two

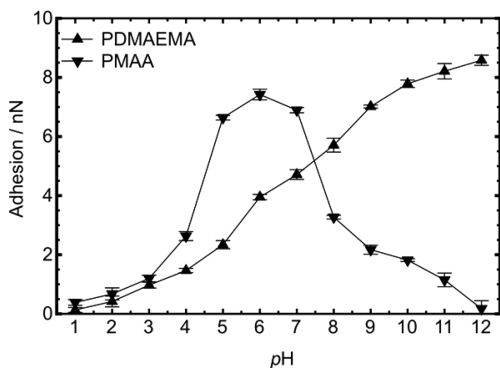


Figure 5. Adhesion results (pull-off force) for the PDMAEMA- and PMAA-coated tips with the PDMAEMA brush on a planar surface.

systems are similar. It is perhaps surprising that the maximum displacement for the PDMAEMA–PDMAEMA system at pH = 12 is well over a micrometer greater than the other results shown in Figure 4, which may indicate that the brush layers (either on the probe, the planar substrate, or both) are being disrupted and pulled off the substrate. By way of contrast, there is no apparent attraction between PMAA and PDMAEMA at pH = 12, except a long-range repulsion, which is likely to be steric as the brushes are being compressed. The adhesion is well illustrated from the histograms shown in Figure 6 presenting the force required to separate the cantilever from the surface.

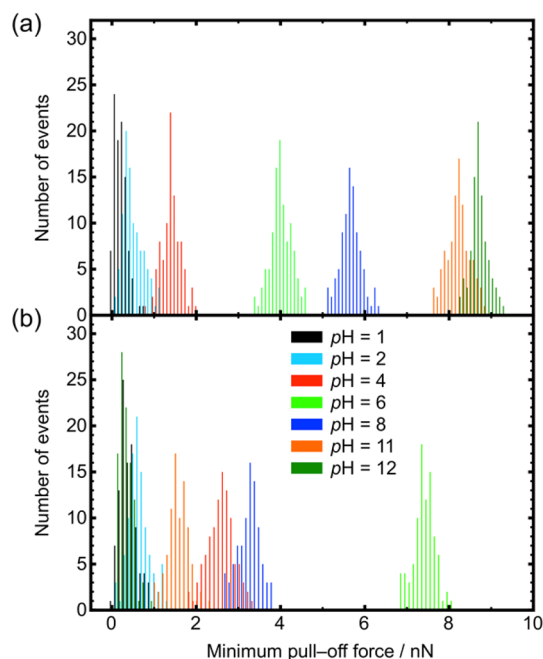


Figure 6. Adhesion histograms for the (a) PDMAEMA- and (b) PMAA-coated tips with the PDMAEMA brush on a planar surface. The legend applies to both histograms.

Here it is clear that the PDMAEMA–PDMAEMA interaction is stronger than that between PDMAEMA and PMAA, with more pH values experiencing relatively strong adhesion.

3.3. Friction. Friction force measurements were performed on the same tip–sample combinations over the same range of pH (1–12), over a scan size of $1\ \mu\text{m} \times 1\ \mu\text{m}$. Friction–load data are shown in Figure 7. For the PDMAEMA–PDMAEMA

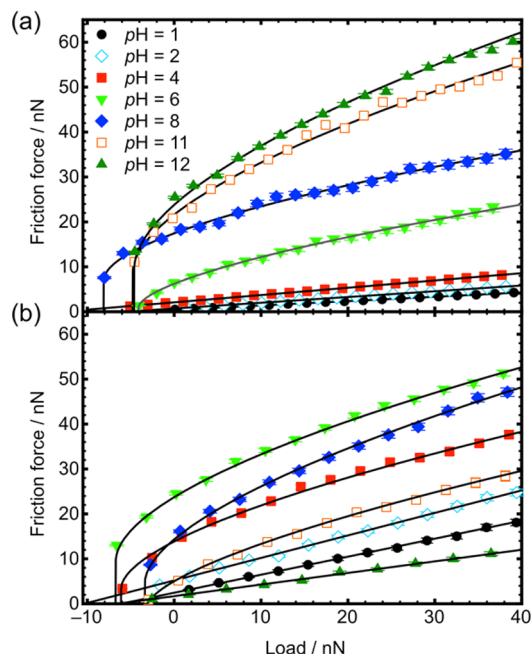


Figure 7. Friction–load plots for the (a) PDMAEMA- and (b) PMAA-coated tips with the PDMAEMA brush on a planar surface. The data were fitted either to a linear friction–load relationship or the JKR or DMT models (nonlinear friction–load relationship).

interaction, the friction force increased with pH across the range of loads studied. At low pH (≤ 4) the friction–load relationship is linear, but at pH = 6 it is nonlinear and it remains so as the pH is increased further. A linear friction–load relationship is associated with nonadhesive sliding, for both polymers and organic monolayers, and represents the limiting case of eq 5, in which the shear term is negligible. When there is energy dissipation through adhesive interactions, the shear term in eq 5 is nonzero and the friction–load relationship becomes nonlinear. Depending on the strength of the adhesive interaction, the contact mechanics may be modeled using either JKR or DMT theory, and the friction–load plots may be fitted using the general transition equation (eq 4).

For the PDMAEMA–PDMAEMA interaction at low pH, protonation of the amine groups is expected, leading to strong solvation of the polymer brushes as well as repulsive interactions between the similar electrostatic charges on the contacting surfaces. As a consequence, adhesive interactions are weak, and the area-dependent term in eq 5 is small; the load-dependent term dominates, yielding a linear friction–load relationship. The main pathways for energy dissipation are via molecular plowing, as was described previously for zwitterionic polymer brushes.¹⁷ As the pH is increased, the degree of protonation of the amine groups on the polymer decreases, with the consequence that the degree of solvation also decreases. At pH 6 the reduction in the degree of surface charge and solvation is such that attractive hydrophobic

interactions between the two surfaces yield a significant adhesive contact. As a result, the area-dependent term in eq 5 makes a significant contribution to the friction force, and behavior that is consistent with DMT mechanics is observed. As the pH increases further, the net adhesive interaction becomes stronger. While plowing contributes to friction, the shear term dominates at high pH when the friction–load relationship is fitted by JKR mechanics.

For the PMAA–PDMAEMA interaction the friction–load relationship is linear at pH = 1, 2, and 12. This indicates that the interaction is dominated by plowing; at either extreme of pH, one of the surfaces (PDMAEMA at pH 1 and 2 and PMAA at pH 12) is ionized and hence highly solvated, leading to a reduction in adhesion. However, the friction–load relationship is nonlinear at pH 4–11, as was the case for frictional behavior of PDMAEMA brushes with AFM tips coated with different monolayers.¹⁵ At these intermediate pH values, the contacting surfaces are partially ionized and solvated to varying degrees; there are net attractive interactions, and the shear term in eq 5 makes a significant contribution to the friction force. The friction force exhibits a maximum around pH = 7. At this pH, the adhesion force is close to its maximum value, probably because the brushes on opposing surfaces contain opposite charges which attract each other strongly. The frictional response of the PDMAEMA-coated tips with PDMAEMA brush films is more lubricious at low pH than that with PMAA brush films at any pH.

4. DISCUSSION

The friction–load behavior for the two polycationic brushes at low pH was fitted to the DMT model ($\alpha = 0$), while at high pH, the behavior was fitted by JKR theory. This is consistent with our knowledge of the charge state of the polymers: at low pH, they are cationic, and electrostatic repulsion causes them to stretch away from the surface. They are also extensively solvated by a substantial quantity of bound water. At higher pH, the polycationic brushes are relatively collapsed, with only a limited quantity of water contained within the layer. The DMT model is thought to apply to stiffer, less adhesive contacts, while the JKR model applies to softer, more adhesive contacts. The analysis of the contact mechanics is thus consistent with our understanding of the respective models: solvation of the brushes at low pH leads to reduced adhesion, and the significant osmotic pressure that results stiffens the brush layer under sliding. During sliding at low pH, the energy dissipation is largely through plowing. As the pH increases, the density of charges in the polymer decreases and the strength of adhesion increases. Although the work of adhesion remains low, the area of contact is large because of the small elastic modulus of a polymer brush layer, which results in a significant contribution of the area-dependent term. As the pH increases still further, and the brush becomes less fully solvated, the contact area increases. The work of adhesion remains low, but the increase in the contact area is equivalent to a reduction in the effective modulus of the contact, leading to a transition from DMT to JKR-type behavior. The interaction of PDMAEMA with a hydrophobic dodecanethiol tip at high pH has also been shown to follow JKR mechanics.¹⁵ In fact, the interaction between PDMAEMA and a hydrophilic silicon nitride tip follows DMT behavior at low pH, so there is consistency between these results and those presented previously.¹⁵

The adhesion of a PMAA-coated tip with PDMAEMA brushes with the tip follows a different pattern, reaching a maximum at pH = 6. A comparison between the respective maximum adhesion results for the PMAA- and PDMAEMA-coated tips allows some conclusions on the relative roles of hydrophobic and electrostatic interactions and noncovalent bonding.

To summarize the results, the following situations are categorized: oppositely charged polyelectrolyte brushes, uncharged polyelectrolyte brushes, similarly charged polyelectrolyte brushes, and brushes whereby one component is charged.

The oppositely charged brushes (PMAA–PDMAEMA) exhibit a maximum adhesion (pull-off force) of 7.4 nN (Figure 5), whereas when both brushes are uncharged (PDMAEMA–PDMAEMA) this is 8.6 nN. In the former case, attractions between opposite electrostatic charges are likely to contribute to the adhesive interaction, but in the latter case, there are no attractive electrostatic interactions and the attractive interactions are largely hydrophobic.

When both polymers have the same charge, a lubricious system with an adhesion of 0.13 nN is observed, which is smaller than any of the results for the PMAA–PDMAEMA system. This small adhesion between the two polycations can only be due to hydrogen bonding or van der Waals interactions. When only one of the components is charged, the adhesion is also weak. This is important because it indicates that hydrogen bonding is not significant in this case.

Hydrogen bonding cannot be considered a possible candidate for the interaction between the two PDMAEMA brushes at high pH because there is no suitable donor group available. Hydrogen bonding is possible between the two polycationic brushes at low pH, when the protonation provides a suitable donor moiety, but the weak pull-off force suggests that it is not contributing significantly. If hydrogen bonding is not contributing to the adhesion in the PDMAEMA–PDMAEMA case, it is perhaps reasonable to conclude that the adhesion between the oppositely charged (PMAA and PDMAEMA) brushes is dominated by electrostatic interactions. In principle, hydrogen bonding is possible over the entire range of pH for the oppositely charged brushes, although if it were significant, the adhesive pull-off force would not decrease as the extremes of pH were approached (Figure 5). Certainly, the repulsive interaction at pH 12 (Figure 4b) is incompatible with hydrogen bonding. However, neutral and charged polymers can exhibit pH-induced reversible adhesion, as has already been demonstrated for the interaction between a poly(acrylic acid) brush and a hydrogel of poly(*N,N*-dimethylacrylamide).²²

The contact mechanics can be presented in the context of the transition parameter, which is plotted in Figure 8. JKR behavior ($\alpha = 1$) is here associated with large adhesion and DMT behavior with smaller adhesion. Linear friction–load behavior (not shown in Figure 8) occurs when adhesion is weak and the area-dependent shear term in eq 5 is small. It is generally the case that DMT behavior is associated with stiff systems. Stiffness is of course relative and perhaps should be compared to the adhesive forces between the surfaces. This is the approach of Tabor, who pointed out that the height of the adhesive neck (i.e., the extension of the contact between two adhesive systems as they are pulled apart) should scale as⁶²

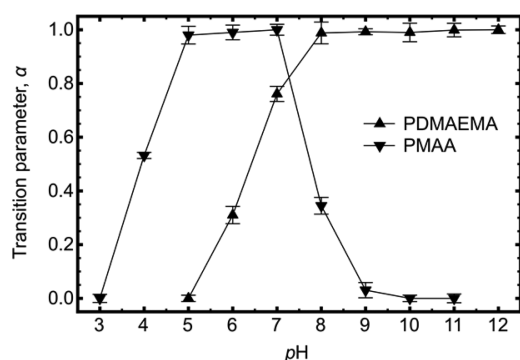


Figure 8. Transition parameter for the PDMAEMA- and PMAA-coated tips with a PDMAEMA surface as a function of pH.

$$h_n \approx \left(\frac{R\gamma^2}{K^2} \right)^{1/3} \quad (7)$$

In the present case, therefore stiffness may also be taken to mean weak adhesion. The cause of the stiffness may be taken to be the solvation of the brush and the weak adhesion due to the resultant osmotic pressure. A collapsed polymer excluding solvent is also expected to be stiff, but PDMAEMA is relatively hydrophilic and is expected to retain some water (although the data in Figure 1 indicate that the amount of water absorbed by the polymer at high pH cannot be large),⁵⁷ and so it is unsurprising perhaps that JKR behavior is observed at high pH for the PDMAEMA-coated tip interacting with the PDMAEMA planar surface. At high pH, PMAA is extended, and so DMT behavior is observed in the interaction with PDMAEMA.

5. CONCLUSIONS

The contact mechanics of polycations and polyanions grafted to an AFM tip with a planar polycationic brush surface have been measured using friction force microscopy. Adhesive interactions demonstrate that the greatest interactions are between the same polycations at high pH and a polycation and polyanion at intermediate pH. The weak interactions between the two polycations at low pH allow the conclusion that hydrogen and van der Waals bonding is largely responsible for the adhesion and electrostatic interactions for the adhesion between oppositely charged polyelectrolytes. The contact mechanics behavior observed for these polyelectrolyte brush systems can be rationalized by treating the friction force as the sum of an area-dependent shear term and a load-dependent plowing term. For highly solvated polycationic brushes, electrostatic repulsions reduce adhesion. Plowing dominates, and the shear term is negligible. As the pH is increased, the polymer becomes less solvated, leading to an increase in the area of contact as the osmotic pressure decreases. As the degree of solvation decreases, the strength of adhesion increases, leading to a transition from behavior consistent with DMT mechanics to behavior that is fitted by JKR theory. For brushes with dissimilar charges, adhesion reaches a maximum around neutral pH, when electrostatic attractions also reach a maximum.

■ ASSOCIATED CONTENT

Supporting Information

The Supporting Information is available free of charge on the ACS Publications website at DOI: 10.1021/acs.macromol.5b01540.

XPS characterization of PMAA brushes (PDF)

■ AUTHOR INFORMATION

Corresponding Author

*E-mail mark.geoghegan@sheffield.ac.uk, fax +44 114 222 3555, tel +44 114 222 3544 (M.G.).

Notes

The authors declare no competing financial interest.

■ ACKNOWLEDGMENTS

The Engineering and Physical Sciences Research Council (EP/F039999/1 and EP/I012060/1) is acknowledged for financial support. Dr. Claire R. Hurley (Sheffield Surface Analysis Centre) is acknowledged for providing the XPS results and Sajjad Tollabimazraehno from Johannes Kepler University Linz, Austria, for carrying out ion-beam milling of probes and SEM imaging of the cantilever.

■ REFERENCES

- Brochard-Wyart, F.; de Gennes, P. G.; Léger, L.; Marciano, Y.; Raphael, E. *J. Phys. Chem.* **1994**, *98*, 9405.
- Geoghegan, M.; Clarke, C. J.; Boué, F.; Menelle, A.; Russ, T.; Bucknall, D. G. *Macromolecules* **1999**, *32*, 5106.
- O'Connor, K. P.; McLeish, T. C. B. *Macromolecules* **1993**, *26*, 7322.
- Chen, M.; Briscoe, W. H.; Armes, S. P.; Klein, J. *Science* **2009**, *323*, 1698.
- Espinosa-Marzal, R. M.; Bielecki, R. M.; Spencer, N. D. *Soft Matter* **2013**, *9*, 10572.
- Klein, J.; Kumacheva, E.; Mahalu, D.; Perahia, D.; Fetters, J. *Nature* **1994**, *370*, 634.
- Nomura, A.; Okayasu, K.; Ohno, K.; Fukuda, T.; Tsujii, Y. *Macromolecules* **2011**, *44*, 5013.
- Collett, J.; Crawford, A.; Hatton, P. V.; Geoghegan, M.; Rimmer, S. J. *R. Soc., Interface* **2007**, *4*, 117.
- Mandal, K.; Balland, M.; Bureau, L. *PLoS One* **2012**, *7*, e37548.
- Azzaroni, O.; Brown, A. A.; Huck, W. T. S. *Adv. Mater.* **2007**, *19*, 151.
- Kobayashi, M.; Takahara, A. *Chem. Rec.* **2010**, *10*, 208.
- Kobayashi, M.; Takahara, A. *Polym. Chem.* **2013**, *4*, 4987.
- Kobayashi, M.; Terada, M.; Takahara, A. *Soft Matter* **2011**, *7*, 5717.
- La Spina, R.; Tomlinson, M. R.; Ruiz-Pérez, L.; Chiche, A.; Langridge, S.; Geoghegan, M. *Angew. Chem., Int. Ed.* **2007**, *46*, 6460.
- Raftari, M.; Zhang, Z.; Carter, S. R.; Leggett, G. J.; Geoghegan, M. *Soft Matter* **2014**, *10*, 2759.
- Sudre, G.; Hourdet, D.; Creton, C.; Cousin, F.; Tran, Y. *Langmuir* **2014**, *30*, 9700.
- Zhang, Z.; Morse, A. J.; Armes, S. P.; Lewis, A. L.; Geoghegan, M.; Leggett, G. J. *Langmuir* **2013**, *29*, 10684.
- Decher, G. *Science* **1997**, *277*, 1232.
- Zhulina, E. B.; Rubinstein, M. *Macromolecules* **2014**, *47*, 5825.
- Angelini, T. E.; Liang, H.; Wriggers, W.; Wong, G. C. L. *Proc. Natl. Acad. Sci. U. S. A.* **2003**, *100*, 8634.
- Retsos, H.; Kiriy, A.; Senkovskyy, V.; Stamm, M.; Feldstein, M.; Creton, C. *Adv. Mater.* **2006**, *18*, 2624.
- Sudre, G.; Olanier, L.; Tran, Y.; Hourdet, D.; Creton, C. *Soft Matter* **2012**, *8*, 8184.
- Carpick, R. W.; Salmeron, M. *Chem. Rev.* **1997**, *97*, 1163.
- Gnecco, E.; Bennewitz, R.; Gyalog, T.; Meyer, E. *J. Phys.: Condens. Matter* **2001**, *13*, R619.
- Grafström, S.; Neitzert, M.; Hagen, T.; Ackermann, J.; Neumann, R.; Probst, O.; Wörtge, M. *Nanotechnology* **1993**, *4*, 143.
- Overney, R.; Meyer, E. *MRS Bull.* **1993**, *18*, 26.
- Frisbie, C. D.; Rozsnyai, L. F.; Noy, A.; Wrigton, M. S.; Lieber, C. M. *Science* **1994**, *265*, 2071.

- 607 (28) Fujihira, M.; Furugori, M.; Akiba, U.; Tani, Y. *Ultramicroscopy*
608 **2001**, 86, 75.
- 609 (29) Leggett, G. J.; Brewer, N. J.; Chong, K. S. L. *Phys. Chem. Chem.*
610 *Phys.* **2005**, 7, 1107.
- 611 (30) Nakagawa, T.; Ogawa, K.; Kurumizawa, T.; Ozaki, S. *Jpn. J. Appl.*
612 *Phys.* **1993**, 32, L294.
- 613 (31) Vezenov, D. V.; Noy, A.; Rozsnyai, L. F.; Lieber, C. M. *J. Am.*
614 *Chem. Soc.* **1997**, 119, 2006.
- 615 (32) Chen, Q.; Kooij, E. S.; Sui, X.; Padberg, C. J.; Hempenius, M.
616 A.; Schön, P. M.; Vancso, G. J. *Soft Matter* **2014**, 10, 3134.
- 617 (33) Mo, Y.; Zhao, W.; Zhu, M.; Bai, M. *Tribol. Lett.* **2008**, 32, 143.
- 618 (34) Sweeney, J.; Webber, G. B.; Rutland, M. W.; Atkin, R. *Phys.*
619 *Chem. Chem. Phys.* **2014**, 16, 16651.
- 620 (35) Limpoco, F. T.; Advincula, R. C.; Perry, S. S. *Langmuir* **2007**,
621 23, 12196.
- 622 (36) Nordgren, N.; Rutland, M. W. *Nano Lett.* **2009**, 9, 2984.
- 623 (37) Wu, Y.; Wei, Q.; Cai, M.; Zhou, F. *Adv. Mater. Interfaces* **2015**, 2,
624 1400392.
- 625 (38) Amontons, G. *Hist. Acad. R. Sci.* **1699**, 206.
- 626 (39) Bhairamadgi, N. S.; Pujari, S. P.; van Rijn, C. J. M.; Zuilhof, H.
627 *Langmuir* **2014**, 30, 12532.
- 628 (40) Pettersson, T.; Naderi, A.; Makuška, R.; Claesson, P. M.
629 *Langmuir* **2008**, 24, 3336.
- 630 (41) Bhairamadgi, N. S.; Pujari, S. P.; Leermakers, F. A. M.; van Rijn,
631 C. J. M.; Zuilhof, H. *Langmuir* **2014**, 30, 2068.
- 632 (42) Landherr, L. J. T.; Cohen, C.; Agarwal, P.; Archer, L. A.
633 *Langmuir* **2011**, 27, 9387.
- 634 (43) Røn, T.; Javakhishvili, I.; Patil, N. J.; Jankova, K.; Zappone, B.;
635 Hvilsted, S.; Lee, S. *Polymer* **2014**, 55, 4873.
- 636 (44) Johnson, K. L.; Kendall, K.; Roberts, A. D. *Proc. R. Soc. London*,
637 *Ser. A* **1971**, 324, 301.
- 638 (45) Derjaguin, B. V.; Muller, V. M.; Toporov, Y. P. *J. Colloid*
639 *Interface Sci.* **1975**, 53, 314.
- 640 (46) Hertz, H. J. *Reine Angew. Math.* **1881**, 92, 156.
- 641 (47) Carpick, R. W.; Ogletree, D. F.; Salmeron, M. *J. Colloid Interface*
642 *Sci.* **1999**, 211, 395.
- 643 (48) Brukman, M. J.; Oncins Marco, G.; Dunbar, T. D.; Boardman,
644 L. D.; Carpick, R. W. *Langmuir* **2006**, 22, 3988.
- 645 (49) Flater, E. E.; Ashurst, W. R.; Carpick, R. W. *Langmuir* **2007**, 23,
646 9242.
- 647 (50) Busuttil, K.; Niko Georgos, N.; Zhang, Z.; Geoghegan, M.;
648 Hunter, C. A.; Leggett, G. J. *Faraday Discuss.* **2012**, 156, 325.
- 649 (51) Niko Georgos, N.; Hunter, C. A.; Leggett, G. J. *Langmuir* **2012**,
650 28, 17709.
- 651 (52) Hutter, J. L.; Bechhoefer, J. *Rev. Sci. Instrum.* **1993**, 64, 1868.
- 652 (53) Ogletree, D. F.; Carpick, R. W.; Salmeron, M. *Rev. Sci. Instrum.*
653 **1996**, 67, 3298.
- 654 (54) Tocha, E.; Song, J.; Schönherr, H.; Vancso, G. J. *Langmuir* **2007**,
655 23, 7078.
- 656 (55) Varenberg, M.; Etsion, I.; Halperin, G. *Rev. Sci. Instrum.* **2003**,
657 74, 3362.
- 658 (56) Aspnes, D. E.; Theeten, J. B.; Hottier, F. *Phys. Rev. B: Condens.*
659 *Matter Mater. Phys.* **1979**, 20, 3292.
- 660 (57) Bütün, V.; Armes, S. P.; Billingham, N. C. *Polymer* **2001**, 42,
661 5993.
- 662 (58) Ruiz-Pérez, L.; Pryke, A.; Sommer, M.; Battaglia, G.; Soutar, I.;
663 Swanson, L.; Geoghegan, M. *Macromolecules* **2008**, 41, 2203.
- 664 (59) Manning, G. S. *J. Chem. Phys.* **1969**, 51, 924.
- 665 (60) Geoghegan, M.; Ruiz-Pérez, L.; Dang, C. C.; Parnell, A. J.;
666 Martin, S. J.; Howse, J. R.; Jones, R. A. L.; Golestanian, R.; Topham, P.
667 D.; Crook, C. J.; Ryan, A. J.; Sivia, D. S.; Webster, J. R. P.; Menelle, A.
668 *Soft Matter* **2006**, 2, 1076.
- 669 (61) Butt, H.-J.; Cappella, B.; Kappl, M. *Surf. Sci. Rep.* **2005**, 59, 1.
- 670 (62) Tabor, D. J. *Colloid Interface Sci.* **1977**, 58, 2.